Journal of Nuclear Materials 404 (2010) 77–81

Contents lists available at ScienceDirect

Journal of Nuclear Materials

journal homepage: www.elsevier.com/locate/jnucmat

The ternary system: silicon–uranium–vanadium

Henri Noel [a], Peter Franz Rogl [b,*]

[a] Laboratoire de Chimie du Solide et Materiaux, UMR-CNRS 6226, Université de Rennes I, Avenue du Général Leclerc, F-35042 Rennes, Cedex, France
[b] Institute of Physical Chemistry, University of Vienna, A-1090 Wien, Währingerstraβe 42, Austria

ARTICLE INFO

Article history:
Received 25 April 2010
Accepted 23 June 2010

ABSTRACT

Phase equilibria in the system Si–U–V were established at 1100 °C by optical microscopy, EMPA and X-ray diffraction. Two ternary compounds were observed, $U_2V_3Si_4$ and $(U_{1-x}V_x)_5Si_3$, for which the crystal structures were elucidated by X-ray powder data refinement and found to be isotypic with the monoclinic $U_2Mo_3Si_4$-type (space group $P2_1/c$; $a = 0.6821(3)$, $b = 0.6820(4)$, $c = 0.6735(3)$ nm, $\beta = 109.77(1)°$) and the tetragonal W_5Si_3-type (space group $I4/mcm$, $a = 1.06825(2)$, $c = 0.52764(2)$ nm), respectively. $(U_{1-x}V_x)_5Si_3$ appears at 1100 °C without any significant homogeneity region at $x \sim 0.2$ resulting in a formula U_4VSi_3 which corresponds to a fully ordered atom arrangement. DTA experiments clearly show decomposition of this phase above 1206 °C revealing a two-phase region $U_3Si_2 + V_3Si$. At 1100 °C U_4VSi_3 is in equilibrium with V_3Si, V_5Si_3, U_3Si_2 and U(V). At 800 °C U_4VSi_3 forms one vertex of the tie-triangle to U_3Si and V_3Si. Due to the rather high thermodynamic stability of V_3Si and the corresponding tie-lines V_3Si + liquid at 1100 °C and V_3Si + U(V) below 925 °C, no compatibility exists between U_3Si or U_3Si_2 and vanadium metal.

1. Introduction

Due to their high melting points well above 2000 °C combined with a remarkable oxidation resistance and good thermal and electrical conductivity, silicides formed by transition metals (T) of the 4th and 5th group have gained considerable attention as high and ultrahigh temperature ceramics. Research particularly focused on the T_5Si_3 compounds and solid solutions among them [1,2]. In recent papers we have shown that ternary systems uranium–transition metal–silicon are characterized by the formation of thermodynamically rather stable high temperature compounds, $U_2M_3Si_4$, which may adopt three different but closely related structure types with variable stoichiometries $U_2Nb_3Si_4$ [3], $U_{2-x}Ti_{3+x}Si_4$ for $0.7 < x < 1.3$ [4] with $Sc_2Re_3Si_4$-type, $U_{2-x}Nb_{3+x}Si_4$, $x = 0.25$ with $Ce_2Sc_3Si_4$-type [3] and $U_2Mo_3Si_4$ with $Y_2Mo_3Si_4$-type [5]. In case of M = Hf a continuous solution $U_xHf_{5-x}Si_4$ of U in binary Hf_5Si_4 (Zr_5Si_4-type) was observed at 1000 °C up to $x \leqslant 1.3$ [6]. Interestingly, although binary Mo_5Si_3 with W_5Si_3-type exists, an independent ternary compound $U_4Mo(Mo_xSi_{1-x})_1Si_2$ was observed [5] extending at 850 °C for $0 < x < 0.33$ and crystallizing with an ordered structure variant of the W_5Si_3-type. The compound was reported to form in a peritectic reaction at 1480 ± 30 °C: $L + U_3Si_2 + U_2Mo_3Si_4 \iff U_4Mo(Mo_xSi_{1-x})Si_2$, $x \sim 0.33$ [5]. In continuation of our research programme on the phase relations and the crystal chemistry in ternary uranium silicide systems, we herein focus on the ternary system with vanadium, for which the result of a cursory investigation was presented in terms of an isothermal section at 600 °C [7], revealing a single ternary compound $U_2V_3Si_4$ with hitherto unknown crystal structure. As far as the phase equilibria and compatibility of U_3Si_2 with V-metal are concerned, the research reported herein is related to low enriched uranium (LEU) proliferation resistant reactor U_3Si_2 dispersion fuels widely used in research reactors [8].

2. Material and methods

About 25 samples, each of a total amount of ca.1 g, were prepared by argon arc melting the elements. Platelets or turnings of depleted uranium (claimed purity of 99.9% Merck, Darmstadt, D), pieces of 6 N-silicon (99.9999%) and vanadium pieces (99.9%, both from Alfa Ventron, Karlsruhe, D) were used as starting materials. The U-metal was surface cleaned in diluted HNO_3 prior to melting. For homogeneity the samples were re-melted several times; weight losses were checked to be altogether less than 0.5 mass%. A part of each alloy was contained within a small alumina crucible, sealed in an evacuated silica tube and heat-treated at 1100 °C for 150 h, respectively and finally quenched by submerging the capsule in cold water. For higher temperatures argon arc melted alloys were heat-treated in a high frequency (HF) furnace (270 kHz) at 1400 °C under argon for 15 h in an alumina crucible within a water-cooled Hukin crucible. Differential thermal analysis was performed in a calibrated Setaram Labsys S60 DTA using alumina crucibles under a stream of argon and heating/cooling rates of 5 K/min. Further details of sample preparation, of the X-ray techniques used (including quantitative Rietveld analyses employing

* Corresponding author. Tel.: +43 1 4277 52456; fax: +43 1 4277 9524.
E-mail address: peter.franz.rogl@univie.ac.at (P.F. Rogl).

0022-3115/$ - see front matter © 2010 Elsevier B.V. All rights reserved.
doi:10.1016/j.jnucmat.2010.06.033

the Fullprof program [9,10]) may be found from our preceding publication on binary uranium silicides [11] or on the ternary system Nb–Si–U [3].

As-cast and annealed samples were investigated by X-ray powder diffraction (XPD), light optical microscopy (LOM) and quantitative electron microprobe analysis (EMPA) on SiC-ground and 1/4 μm diamond paste polished surfaces. A Jeol energy dispersive X-ray microanalyser (EMPA-XMA) was used for proper identification of the phases operating at an acceleration voltage of 15 kV at 20 nA sample current using the U-Mα, V-Kα and Si-Kα radiation. X-ray intensities were corrected for ZAF effects.

3. Results and discussion

3.1. The binary boundary systems

The boundary systems, V–U and Si–V, were accepted from the compilation of binary alloy phase diagrams by Massalski [12]. The U–Si system used herein is from a reinvestigation by the authors [11,13,14], but the uranium-rich part of the diagram up to 4 at.% Si is taken from Straatmann and Neumann [15] and from Holleck and Kleykamp [16]. Crystallographic data of the boundary phases are listed in Table 1 [16,17].

3.2. Phase relations at 1100 °C and 1400 °C

Phase relations within the Si–U–V ternary system were established for the isothermal section at 1100 °C (shown in Fig. 1) and confirm the ternary compound τ_1 close to the composition $U_2V_3Si_4$. From optical microscopy, from variation of lattice parameters and particularly from EMP-analyses, $U_2V_3Si_4$ is observed at its stoichiometric composition without a significant homogeneous region. The composition of τ_1 is located well within the large field of primary crystallization of V_5Si_3. Thus τ_1 does not melt congruently but forms at high temperature presumably via a peritectic reaction $L + U_3Si_5 + V_5Si_3 = U_2V_3Si_4$ (see microstructure in Fig. 2). In line with the high stability of the tie-line $U_3Si_2 + V_5Si_3$ (see micrograph in Fig. 3), the compound $U_2V_3Si_4$ is in equilibrium with the modifications of U_3Si_5 (AlB_2-type derivatives) but not with USi_{2-x} ($ThSi_2$, $GdSi_2$-types) which ties to V_5Si_3. Phase relations are documented in the microstructures of a set of selected alloys in Figs. 3–5. Phase equilibria within the concentrational field U_3Si_2–V_5Si_3–Si were found to persist at 1400 °C.

At lower silicon concentrations X-ray spectra reveal the formation of a ternary compound U_4VSi_3 (for crystallographic details see below) in a series of alloys from the region U_3Si_2–V_3Si–(U) which were annealed between 800 °C and 1150 °C (see micrographs in Figs. 3–5). DTA of a sample U_3VSi_2, which was arc melted and annealed at 800 °C, clearly reveals the incongruent decomposition of U_4VSi_3 at 1206 °C on heating (see Fig. 6). At 1100 °C U_4VSi_3 was observed to enter equilibria with V_5Si_3, V_3Si, U_3Si_2 and U-rich liquid.

Due to the rather high thermodynamic stability of V_3Si, the tie-lines (i) V_3Si + liquid at 1100 °C and (ii) $V_3Si + U_3Si + U(V)$ below 925 °C prevent compatibility for the join U_3Si_2–V(U). The three-phase condition of sample $U_{33}V_{55}Si_{22}$ at 850 °C, 1100 °C and 1400 °C yields the absence of a ternary Laves type phase '$U(V,Si)_2$' as typical for Cr- and Mn-containing systems [18,19]. Mutual solubility of U-silicides and V-silicides in alloys annealed at 1100 °C are found to be very small i.e. below about 0.6 at.% V (see also EPMA data given at the various micrographs). The equilibrium between U_3Si_2 and V_5Si_3 is in contrast to a tie-line U(M) + τ_1-$U_2M_3Si_4$ as usually observed in ternary systems U-M-Si where M = Ti, Zr, Hf, Nb, Mo (for details see references given in Section 1).

3.3. The crystal structures of $U_2V_3Si_4$ and U_4VSi_3

3.3.1. $U_2V_3Si_4$

Room temperature X-ray powder patterns of $U_2V_3Si_4$ alloys, annealed in an HF furnace under argon and quenched from about 1400 °C, were successfully indexed on the basis of a monoclinic unit cell (Table 2). Extinctions were observed only for the screw axis 2_1 and the c-glide: (0 *k* 0) (*h* 0 l) extinct for $k = 2n + 1$ and $l = 2n + 1$, respectively, and thus are compatible with $P2_1/c$ as the

Table 1
Crystallographic data of binary boundary phases of the system Si–U–V.

Phase	Pearson symbol	Space group	Prototype	Lattice parameter in nm			Remarks	References
				a	*b*	*c*		
γU	cI2	$Im\bar{3}m$	W	0.3524 0.35335			1132.3–774.8 °C, at 787 °C	[12,16,17]
βU	tP30	$P4_2/mnm$	βU	1.0759 1.07589		0.5656 0.56531	774.8–667.7 °C, at 682 °C	[12,16,17]
αU	oC4	Cmcm	αU	0.28537	0.58695	0.49548	<667.7 °C	[12,16]
V	cI2	$Im\bar{3}m$	W	0.330256			<1910 °C, at 299 K	[12,17]
Si	cF8	$Fd\bar{3}m$	$C_{diamond}$	0.543065			<1414 °C	[12]
V_3Si	cP8	$Pm\bar{3}n$	Cr_3Si	0.4727		1.0562	<1925 °C	[12,17]
V_5Si_3	tI32	*I*4/*mcm*	W_5Si_3	0.9429		0.4757	2010 °C	[12,17]
V_6Si_5	oI44	Ibam	V_6Si_5	0.4858	1.5966	0.4858	1670–1160 °C	[12,17]
VSi_2	hP9	$P6_222$	$CrSi_2$	0.4562	–	0.6359	<1677 °C	[12,17]
γU_3Si	cP4	$Pm\bar{3}m$	Cu_3Au	0.4346			930–759 °C	[12,24]
βU_3Si	tI16	*I*4/*mcm*	βU_3Si	0.60328		0.86907	762 to −153 °C	[15,17]
αU_3Si	oF32	Fmmm	αU_3Si	0.8654	0.8549	0.8523	<−153 °C, at −193 °C	[15,17]
U_3Si_2	tP10	P4/mbm	U_3Si_2	0.73299		0.39004	<1665 °C	[12,17]
U_5Si_4	hP36	P6/mmm	$U_{20}Si_{16}C_3$	1.0467		0.7835		[14]
USi	tI38	*I*4/mmm	USi	1.058		2.431	<1580 °C	[13]
USi[a]	oP8	Pnma	FeB	0.7585	0.3903	0.5663		[25]
U_3Si_5	hP3	P6/mmm	AlB_2	0.3843		0.4069	<1770 °C	[12]
U_3Si_5(o1)	oP6	Pmmm	dist. AlB_2	0.3869	0.6660	0.4073	at 63 at.%Si	[11]
U_3Si_5(o2)	oP6	Pmmm	dist. AlB_2	0.3893	0.6717	0.4042	at ~63 at.%Si	[11]
USi_{2-z}	oI12	Imma	def. $GdSi_2$	0.3953	0.3929	1.3656	at 64 at.%Si	[11]
USi_{2-z}	tI12	$I4_1/amd$	def. $ThSi_2$	0.39423		1.3712	<1710 °C at 65 at.%Si	[11,12]
USi_2	tI12	$I4_1/amd$	$ThSi_2$	0.3922		1.4154	<450 °C	[12,17]
USi_3	cP4	$Pm\bar{3}m$	Cu_3Au	0.4060			<1510 °C	[12]
τ_1-$U_2V_3Si_4$	mP18	$P2_1/c$	$U_2Mo_3Si_4$	0.6821(3)	0.6820(4)	0.6735(3)	β = 109.77(1)°	This work
τ_2-U_4VSi_3	tI32	*I*4/*mcm*	W_5Si_3	1.06825(2)	1.06825(2)	0.52764(2)	–	This work

[a] Probably oxygen stabilized [11].

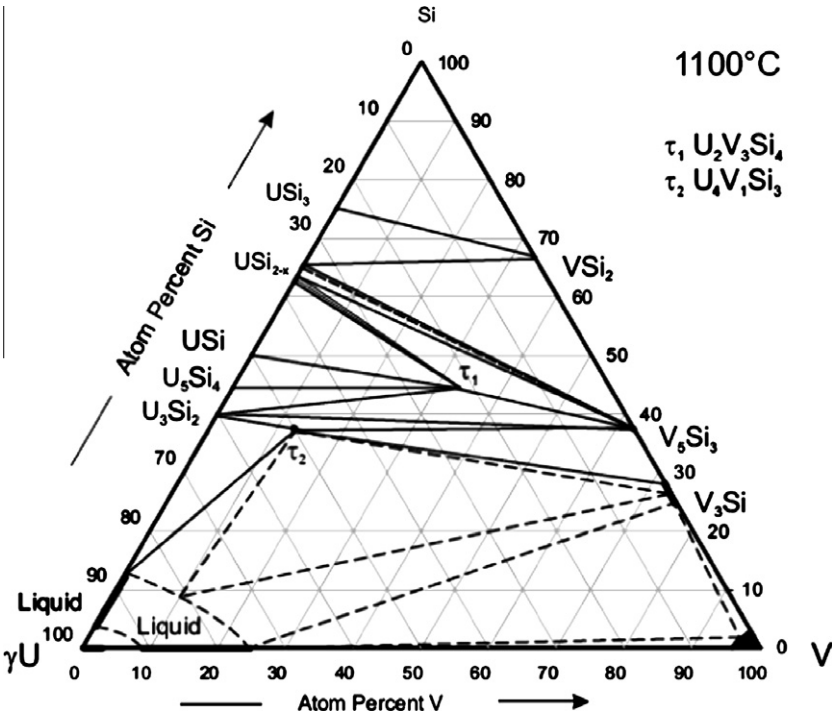

Fig. 1. System V–Si–U; isothermal section at 1100 °C.

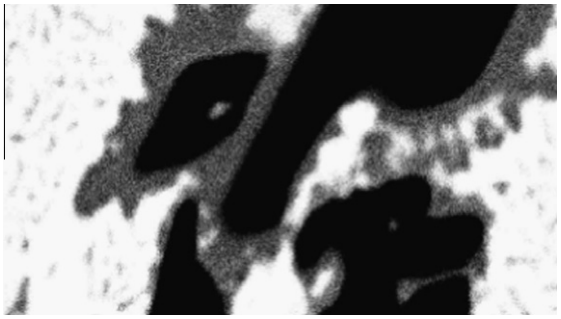

Fig. 2. EMPA-backscatter image of the alloy $U_2V_3Si_4$ annealed at 1100 °C for 150 h: dark crystals $U_{0.3}V_{62.5}Si_{37.2}$ (V_5Si_3), bright regions $U_{42.0}V_{0.7}Si_{57.3}$ (U_3Si_5); grey particles $U_{22.2}V_{34.1}Si_{43.7}$ ($U_2V_3Si_4$).

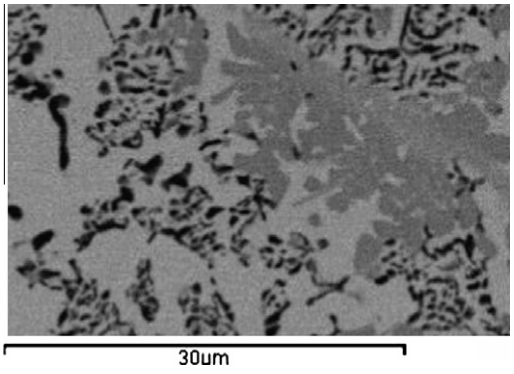

Fig. 4. EMPA-backscatter image of the alloy U_2VSi_2 annealed at 1000 °C for 150 h: black crystals V_5Si_3, grey regions $U_{24}V_{34}Si_{42}$ ($U_2V_3Si_4$); bright matrix $U_{61}V_{0.3}Si_{38.7}$ (U_3Si_2).

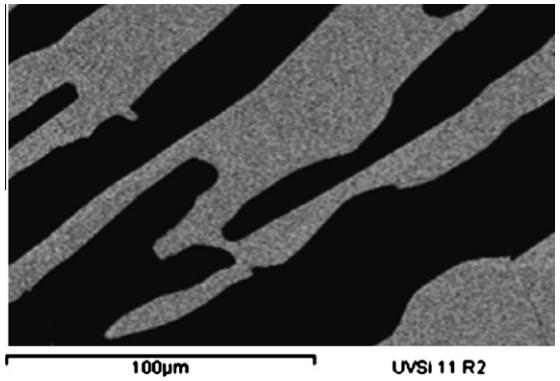

Fig. 3. EMPA-backscatter images of the alloy U_3VSi_2 annealed at 1400 °C for 5 h: black crystals $U_{0.2}V_{60.8}Si_{39.0}$ (V_5Si_3), grey matrix $U_{60.3}V_{0.44}Si_{39.3}$ (U_3Si_2).

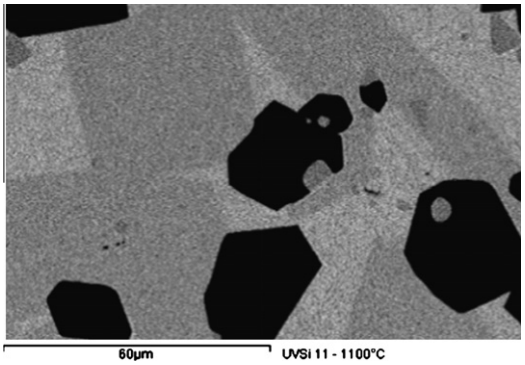

Fig. 5. EMPA-backscatter image of the alloy U_3VSi_2 annealed at 1100 °C for 150 h: black crystals $U_{0.1}V_{74.5}Si_{25.4}$ (V_3Si), grey regions $U_{50.1}V_{12.9}Si_{37.0}$ (U_4VSi_3); bright matrix (U,V).

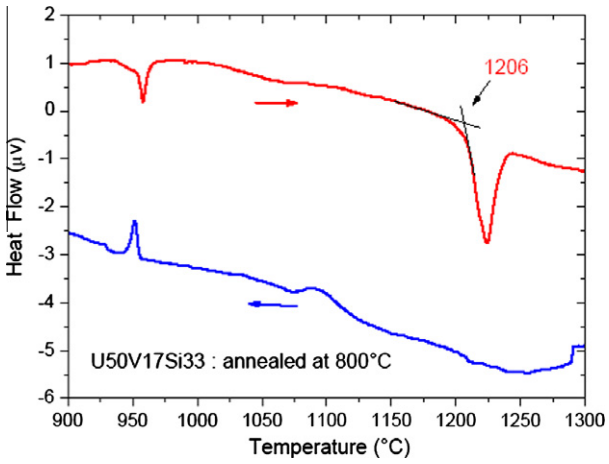

Fig. 6. DTA record on a sample U_3VSi_2 at a heating and cooling rate of 5 K/min. The prominent endothermal peak in heating with a sluggish onset at 1206 °C reveals the decomposition of U_4VSi_3. Slow reaction kinetics hinders a corresponding exothermic peak on cooling.

highest symmetric space group. The chemical formula, unit cell dimensions, crystal symmetry and X-ray intensities all strongly suggest isotypism with the ordered $U_2Mo_3Si_4$-type [20]. Assuming the atom order and the atom parameter set of $U_2Mo_3Si_4$, a full matrix–full profile Rietveld refinement of a Siemens D5000 flat specimen intensity recording satisfactorily converged at a reasonably low residual value $R_F = 0.057$ (Table 2) and with only slightly modified atom parameters. The alloy contained minor amounts of U_3Si_5 (AlB_2-type) and V_5Si_3 (W_5Si_3-type), which were included in the refinement. Occupancies in $U_2V_3Si_4$ have been refined for all atom sites revealing no deviation from the atom distribution given. Due to the usually strong correlation between occupational and thermal parameters, the isotropic temperature coefficients were individually analysed and kept constant throughout the refinement. The final structure and profile parameters and the reliability values obtained from the least squares refinements are presented in Table 2. Data in Table 2 were made consistent with a standardized setting of the atom positions employing the program Structure Tidy [21]. Interatomic U–U distances, $d_{U-U} = 0.3363$ and 0.3560 nm, are below and near the Hill limit ($d_{U-U} = 0.350$ nm) [22].

3.3.2. U_4VSi_3

X-ray powder patterns of alloys, U_3VSi_2, U_4VSi_3 and $U_{51}V_{15}Si_{34}$, annealed at temperatures between 800 and 1100 °C, revealed an intensity pattern related to the W_5Si_3-type. Indexation of the relevant peaks, prompted a tetragonal cell (see Table 1), however, unit cell dimensions were significantly larger and intensities significantly different than those of binary V_5Si_3 with the W_5Si_3-type. The situation resembled the phase $U_4Mo(Mo_xSi_{1-x})Si_2$ ($0 < x < 0.3$ at 850 °C) which also adopted a partially ordered structure variant of the W_5Si_3-type [5]. The new phase was obtained in practically single-phase condition in the alloys U_3VSi_2 after annealing at 800 °C (minor amounts of U_3Si) and in U_4VSi_3 after annealing at 1050 °C (minor amounts of V_3Si). Rietveld refinements prompted a complete atom order as typical for the atom site distribution of U_4VSi_3 and satisfactorily converged at a reasonably low residual value $R_F = 0.069$ (Table 2) with atom parameters only slightly modified with respect to isotypic U_4MoSi_3 [5]. As lattice parameter variation in the surrounding alloys was very small, the new phase was assumed to exist at the stoichiometric composition U_4VSi_3 without any significant homogeneity region. Interatomic distances reveal tight bonding in the V/Si clusters but with a rather wide spread of U–U contacts, $0.27 < d_{U-U} < 0.37$ nm. The extremely short bonds, ranking among the shortest known contacts in uranium intermetallics ($d_{U-U} = 0.275$ nm in αU; $d_{U-U} = 0.278$ nm in U_2Ti; $d_{U-U} = 0.284$ nm in $U(Co,Si)_2$, etc. [17]), imply a high degree of 5f orbital overlap in favour of nonmagnetic uranium–uranium interactions. It is interesting to note that a W_5Si_3-type compound forms in the U-rich ternary although isotypic binary V_5Si_3 exists with only a minor solid solubility for uranium. A similarly ordered structure variant was encountered for Pu_4CeCo_3 [23].

4. Conclusion

Phase equilibria in the system Si–U–V are characterized by two ternary compounds: τ_1-$U_2V_3Si_4$ and τ_2-U_4VSi_3, which both form in

Table 2
Crystallographic data of $U_2V_3Si_4$ and U_4VSi_3 from X-ray Rietveld powder refinement. Crystal structure data standardized with program structure Tidy [21].

Parameter/compound[a]	$U_2V_3Si_4$	U_4VSi_3
Composition, EMPA	$U_{22.2}V_{34.1}Si_{43.7}$	–
Composition from refinement[b]	$U_2V_3Si_4$	U_4VSi_3
Space group	$P2_1/c$; No. 14	$I4/mcm$, No. 140
Structure type	$U_2Mo_3Si_4$	Ordered W_5Si_3
a, b, c [nm]	0.6821(3), 0.6820(4), 0.6735(3)	1.06845(2), 1.06845(2), 0.52782(2)
Beta [°]	$\beta = 109.77(1)°$	–
Reflections measured	325	109
Number of variables	19	26
$R_F = \Sigma\lvert F_o - F_c\rvert/\Sigma F_o$	0.057	0.069
$R_I = \Sigma\lvert I_o - I_c\rvert/\Sigma I_o$	0.083	0.098
$R_{wP}=[\Sigma w_i\lvert y_{oi} - y_{ci}\rvert^2/\Sigma w_i\lvert y_{oi}\rvert^2]^{1/2}$	0.098	0.114
$R_P = \Sigma\lvert y_{oi} - y_{ci}\rvert/\Sigma\lvert y_{oi}\rvert$	0.070	0.127
$R_e = [(N-P+C)/\sum w_i y_{oi}^2]^{1/2}$	0.019	0.071
Atom parameters		
U in 4e (x, y, z); occ = 1.0	0.6861(2); 0.3348(2); 0.0589(2)	U in 16k ($x, y, 0$); occ = 1.0 $x = 0.0941(2)$, $y = 0.2280(2)$
B_{iso} (10^2 nm^2)	0.22(3)	B_{iso} (10^2 nm^2) = 0.59(3)
V1 in 2d (0,0,0); occ = 1.0	0;0;0	V in 4b (0, ½, ¼); occ = 1.0
B_{iso} (10^2 nm^2)	0.27(5)	B_{iso} (10^2 nm^2) = 0.35(4)
V2 in 4e (x, y, z); occ = 1.0	0.2555(4); 0.3309(6); 0.2482(6)	Si1 in 8h (x, ½ + x, 0); occ = 1.0 $x = 0.1465(2)$
B_{iso} (10^2 nm^2)	0.27(5)	B_{iso} (10^2 nm^2) = 0.27(5)
Si1 in 4e (x, y, z); occ = 1.0	0.4098[a]; 0.0457; 0.3686	Si2 in 4a (0, 0, ¼); occ = 1.0
B_{iso} (10^2 nm^2)	0.97(3)	B_{iso} (10^2 nm^2) = 0.27(5)
Si2 in 4e (x, y, z); occ = 1.0	0.0037[a]; 0.1332; 0.3673	–
B_{iso} (10^2 nm^2)	0.95(3)	

[a] Atom parameters kept fixed during refinement.

incongruent reactions. The crystal structures of these compounds were elucidated by X-ray powder Rietveld refinements: τ_1-$U_2V_3Si_4$ crystallizes with the $U_2Mo_3Si_4$-type (space group $P2_1/c$) whereas τ_2-U_4VSi_3 is isotypic with the tetragonal W_5Si_3-type (space group $I4/mcm$). DTA experiments clearly show for τ_2-U_4VSi_3 decomposition on heating above 1206 °C. At 800 °C U_4VSi_3 is one vertex of the tie-triangle to U_3Si and V_3Si. Due to the equilibrium tie-lines V_3Si + U(V) and U_4VSi_3 + U(V) no compatibility exists between U_3Si or U_3Si_2 and vanadium metal.

Acknowledgements

Support by the French–Austrian Bilateral Scientific Technical Exchange Programme "Amadee", Project FR10/2008, is gratefully acknowledged.

References

[1] C.J. Rawn, J.H. Schneibel, C.L. Fu, Acta Materialia 53 (8) (2005) 2431–2437.
[2] L. Cretegny, B.P. Bewlay, A.M. Ritter, M.R. Jackson, in: MRS Symposium Proceedings, vol. 842, 2005, pp. 273–278.
[3] T. LeBihan, H. Noël, P. Rogl, J. Nucl. Mater. 277 (2000) 82.
[4] F. Weitzer, H. Noël, P. Rogl, J. Alloys Compd. 350 (2003) 155.
[5] P. Rogl, T. LeBihan, H. Noël, J. Nucl. Mater. 288 (2001) 66.
[6] F. Weitzer, P. Rogl, H. Noël, J. Alloys Compd. 387 (2005) 246.
[7] O. Sologub, P. Salamakha, in: Abstract of a Paper at 29iemes Journées des Actinides, May 14–17, 1999, Luso, Portugal, pp. 117.
[8] U.S. Nuclear Regulatory Commission Report, NUREG-1313, July 1988.
[9] J. Rodriguez-Carvajal, Physica B 192 (1993) 55.
[10] T. Roisnel, J. Rodriguez-Carvajal, WinPLOTR, a tool to plot powder diffraction patterns. Laboratoire Leon Brillouin (CEA-CNRS) France (1998).
[11] K. Remschnig, T. LeBihan, H. Noël, P. Rogl, J. Solid State Chem. 97 (1992) 391.
[12] T.B. Massalski, in: Binary Alloy Phase Diagrams, second ed. ASM International, Materials Park, OH, 1990.
[13] T. LeBihan, Thesis, Université de Rennes, France (1993) pp. 1–194.
[14] H. Noël, V. Queneau, J.P. Durand, P. Colomb, in: Abstract of a Paper at Int. Conf. on Strongly Correlated Electron Systems – SCES98, 15-18 Juillet, Paris, 1998, p. 92.
[15] J.A. Straatmann, N.F. Neumann, Equilibrium structure in the high uranium silicon alloy system, USAEC Report MCW-1486, Malinckrodt Chemical Works, October 23 (1964), cited in React. Mater. 8(2) (1965) 57–73.
[16] H. Holleck, H. Kleykamp, Gmelin Handbook of Inorganic Chemistry, Uranium, Supplement, vol. C12, Springer, New York, 1987, pp. 1–279.
[17] P. Villars, L.D. Calvert, Pearson's Handbook of Crystallographic Data for Intermetallic Phases, second ed., ASM International, Materials Park, Ohio, 1991.
[18] T. LeBihan, J.C. Levet, H. Noël, J. Solid State Chem. 121 (1996) 479.
[19] Yu. Kuzma, H. Nowotny, Monatsh. f. Chemie, 95 (1964) 1219.
[20] M. Sikiritsa, L.G. Akselrud, Y.P. Yarmolyuk, The crystal structure of the compound $U_2Mo_3Si_4$, in: Abstracts of the 3rd All-Union Conference on the Crystallochemistry of Intermetallic Compounds (in Russian), Vishcha Skhola, L'viv, 1978, p.11.
[21] E. Parthé, L. Gelato, B. Chabot, M. Penzo, K. Cenzual, R. Gladyshevskii, TYPIX Standardized Data and Crystal Chemical Characterization of Inorganic Structure Types, Springer, Berlin, Heidelberg, 1994.
[22] H.H. Hill, in: Plutonium 1970 and Other Actinides, ed. W.N. Miner, Nuclear Metallurgy, vol. 17 (AIME), NY (1979) p. 2.
[23] A.C. Larson, R.B. Roof Jr, D.T. Cromer, Acta Crystallogr. 17 (1964) 1382.
[24] Z.M. Alekseeva, J. Nucl. Mater. 186 (1992) 294.
[25] W.H. Zachariasen, Acta Crystallogr. 2 (1949) 94.